Journal of Solid State Chemistry **147,** 170–176 (1999)
Article ID jssc.1999.8208, available online at http://www.idealibrary.com on IDEAL®

Composite Copper Chalcogenide Halides: Neutron Powder Diffraction of $CuClCu_2TeS_3$ and Electrical Properties of $CuClCu_2TeS_3$, $(CuI)_2Cu_3SbS_3$, and $(CuI)_3Cu_2TeS_3$

Arno Pfitzner,[1] Sara Reiser, and Tom Nilges

Anorganische Chemie, Universität Siegen, D-57068 Siegen, Germany
E-mail: pfitzner@chemie.uni-siegen.de

and

Winfried Kockelmann

Mineralogisch-Petrologisches Institut, Universität Bonn, c/o Rutherford Appleton Laboratory, ISIS, Chilton, Didcot, Oxon OX11 0QX, United Kingdom
E-mail: W.Kockelmann@rl.ac.uk

Received November 4, 1998; in revised form February 1, 1999; accepted February 5, 1999

IN MEMORIAM JEAN ROUXEL

The crystal structure of $CuClCu_2TeS_3$ was refined from TOF neutron powder diffraction data in order to verify the distribution of chlorine and sulfur. It is a novel derivative of the zincblende type with an ordered distribution both of the cations Cu^+ and Te^{4+} and of the anions Cl^- and S^{2-}. The compound crystallizes in the rhombohedral system, space group *R3m* (No. 160) with $a = 7.3502(1)$ Å, $c = 10.3873(2)$ Å, $V = 485.99$ Å^3, and $Z = 3$. The structure refinement converged to $R_{wp} = 0.039$ and $R_{Bragg} = 0.032$. From the neutron data it can be derived that there is no significant disorder of Cl and S atoms. Impedance spectroscopic measurements in the temperature range 140–280°C reveal that $CuClCu_2TeS_3$ is a semiconductor with an activation energy of 0.75 eV ($T < 200$°C) and 1.25 eV ($T > 200$°C), respectively. On the other hand $(CuI)_3Cu_2TeS_3$ and $(CuI)_2Cu_3SbS_3$ exhibit high copper ion conductivity with activation energies of 0.2 and 0.35 eV, respectively, but a negligible electronic conduction.

INTRODUCTION

Copper(I) halides and chalcogenides are well known to show high copper ion conductivity at elevated temperatures whereas a mixed electronic and ionic conductivity is discussed for the room temperature region. In order to synthesize new materials with high copper ion conductivity it therefore seems desirable to elucidate the existence of copper halide and copper chalcogenide-based composite compounds. Recently it was shown that adducts of copper(I) halides to *neutral* polymers of main group elements, e.g., $(CuI)_8P_{12}$ and $(CuI)_3P_{12}$, are a promising group of novel copper ion conducting materials (1–3). However, materials based on mixed copper halides and chalcogenides might provide an even higher conductivity since the polarizibility of a mixed halide chalcogenide anionic framework is supposed to be higher than that of compounds containing *neutral* bonding partners attached to the copper ions. Since the systems CuX–Cu_2Q (X = halide, Q = chalcogenide) show large miscibility gaps between the end-member phases (4–6) we started to inspect the systems CuX–$Cu_mM^{(6-m)+}S_3$ (with M = Sb, Te) for the existence of new composite materials. The sulfide end-members of these systems are Cu_3SbS_3 and "Cu_2TeS_3." Whereas the crystallography and polymorphism of Cu_3SbS_3 including a high-temperature phase with a pronounced copper disorder and a high copper diffusion coefficient is well established (7–10), a compound with the exact composition Cu_2TeS_3 is not yet known. However, a phase with the composition $Cu_{17.6}Te_8S_{26}$, which is close to $8 \times Cu_2TeS_3$, was synthesized recently (11). These solids contain complex thiometalate ions and therefore belong to the group of the so-called sulfosalts. In order to show up the composite character of the compounds under discussion the copper halide "part" and the copper thiometalate "part" of them are separated in the chemical formulas. $(CuI)_3Cu_2TeS_3$ (12), $(CuI)_2Cu_3SbS_3$ (13), and $CuClCu_2TeS_3$ (14) are the first examples we obtained in this series. They all consist of one formula unit of a copper thiometallate combined with a different amount of a copper halide, namely,

[1] To whom correspondence should be addressed.

0022-4596/99 $30.00

copper iodide and copper chloride, respectively. Using copper(I) bromide as a starting material the product did not contain $[TeS_3]^{2-}$ ions but instead an unforeseen compound with $TeS_2^{\bullet -}$ radical anions emerged (15). The copper bromide homologue of $(CuI)_2Cu_3SbS_3$ turned out to be metastable because it rapidly decomposes yielding $SbBr_3$ and other products at elevated temperatures (16). The crystal structure of $CuClCu_2TeS_3$ was recently determined by X-ray methods but due to their almost equal scattering power the distribution of Cl^- and of S^{2-} could only be derived from crystal chemical considerations (14). Therefore, a refinement of the structure using neutron diffraction data is desirable in order to verify the crystal structure. A detailed knowledge of the crystal structures of the compounds under discussion is necessary for a better understanding of their electrical properties, and especially their ionic conductivity. Here we report on time-of-flight (TOF) neutron powder diffraction studies of $CuClCu_2TeS_3$, and discuss the electrical properties of $CuClCu_2TeS_3$, $(CuI)_3Cu_2TeS_3$, and $(CuI)_2Cu_3SbS_3$ with respect to their crystal structures.

EXPERIMENTAL

Preparation and Characterization

The title compounds were obtained by reaction of mixtures of appropriate amounts of the corresponding copper halide, copper, sulfur, and tellurium or antimony. The starting mixtures were sealed in evacuated silica ampoules, homogenized by melting and subsequent grinding, and then kept about 50 degrees below their decomposition temperatures. After some weeks pure microcrystalline samples containing also single crystals suitable for a structure determination were obtained. Preparational details are given elsewhere (12–14). Prior to further investigation, the purity of the samples was checked by X-ray powder diffraction with a Siemens D5000 diffractometer (Cu$K\alpha_1$ radiation, Si as external standard). Thermal analyses were performed with a computer-controlled Linseis L62 DTA cell.

Conductivity Measurements

The electrical properties of the title compounds were determined from cold-pressed pellets of finely ground microcrystalline samples which were contacted by gold foils and platinum wires. Impedance measurements were performed with a Zahner IM6 impedance analyzer and a homemade spring-loaded measuring cell (3). After an equilibration time of 60 min impedance spectra were recorded in the frequency range 100 mHz to 4 MHz. The samples were permanently kept under an atmosphere of purified Ar gas during the temperature-dependent measurements.

Neutron Powder Diffraction

Neutron diffraction measurements of $CuClCu_2TeS_3$ were performed on the ROTAX time-of-flight diffractometer (17) at the ISIS spallation neutron source of the Rutherford Appleton Laboratory, United Kingdom. The powder sample was contained in a vanadium can of 11 mm diameter. Data were collected at ambient temperature using two position-sensitive detector banks at 2Θ angles of 28° and 125°, respectively, providing a range of accessed d-spacings from 0.3 to 15.0 Å. The data collection time was about 10 h.

The diffraction data were analyzed using the Rietveld program of the General Structure Analysis System (GSAS) (18), see Table 1. The neutron scattering lengths used were $b_{Cu} = 0.773 \times 10^{-12}$ cm, $b_{Cl} = 0.959 \times 10^{-12}$ cm, $b_{Te} = 0.58 \times 10^{-12}$ cm, and $b_S = 0.2847 \times 10^{-12}$ cm. The following structure parameters were refined: unit cell constants, positional parameters, isotropic displacement parameters, and occupation fractions of sites 3*a* and 9*b* with chlorine and sulfur, respectively. The occupancies were constrained according to the composition of the $CuClCu_2TeS_3$ formula unit. Refined diffraction patterns are displayed in Fig. 1. From the refinement of the occupational parameters of chlorine and sulfur it became evident that there is no significant disorder of these two elements detectable. Thus, the R values dropped to a minimum for the model already obtained by single-crystal X-ray methods, see Table 2.

STRUCTURAL RESULTS AND DISCUSSION

The crystal structure of $CuClCu_2TeS_3$ is a novel ordered zincblende variant (14). The structural data obtained by

TABLE 1
Experimental Details for the Neutron Powder Diffraction Measurement

	Bank 1 Forward scattering	Bank 2 Backscattering
Instrument parameters		
Target–sample distance	13995 mm	13995 mm
Sample–detector distance	1140 mm	1230 mm
2Θ angle of detector	28.12°	125.5°
Wavelength band	0.5–5.2 Å	0.5–5.2 Å
d-spacing range accessible	0.7–15 Å	0.3–2.8 Å
Medium resolution $\Delta d/d$	0.015	0.004
Rietveld parameters		
d-spacing range used	0.9–7 Å	0.6–3.0 Å
No. of reflections	150	330
No. of structure parameters	12	12
Type of profile function	Double-exponential-Voigt	Double-exponential-Voigt
No. of profile parameters	3	3
No. of background parameters	10	16

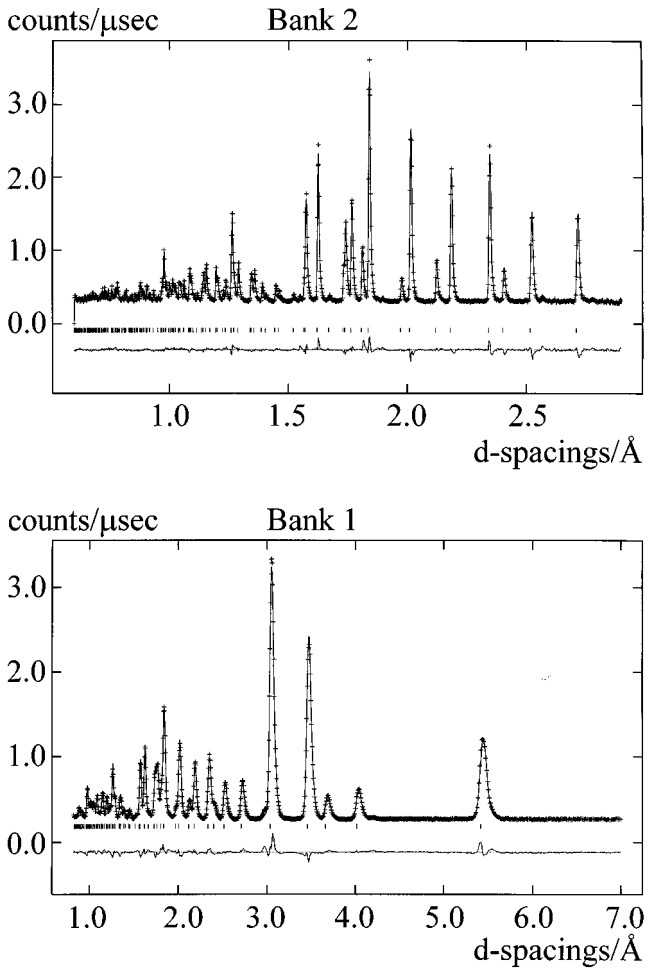

FIG. 1. TOF neutron powder pattern of $CuClCu_2TeS_3$. The *d*-spacing range is 0.6–3.0 Å for bank 2 and 0.7–15.0 Å for bank 1. (+) Measured intensity; (—) calculated intensity; (|) calculated reflection positions.

X-ray diffraction and neutron powder diffraction do not show any significant differences (see Table 2). A slight discrepancy concerning the lattice parameters has to be notified. Since the data obtained by X-ray powder and single-crystal methods are equal within their ESDs this discrepancy might be either due to a slightly different temperature during the data collection or a small misalignment of the sample during the neutron diffraction measurement. From Fig. 2 and the atomic positions displayed in Table 2 a significant distortion of the structure as compared to the regular zincblende structure type becomes obvious. This distortion is due to an excess of two valence electrons per formula unit. The number of valence electrons is 34 but should be 32 for eight atoms in a regular tetrahedral structure. A fourfold coordination of copper and sulfur results, whereas tellurium and chlorine have a coordination number of 3. The two excess electrons thus "cut" one regular bond and two lone electron pairs result. They are located at the tellurium and at the chlorine atom. A detailed crystallographic description of the structure of $CuClCu_2TeS_3$ and its relation to the zincblende type is already given in Ref. (14).

For $(CuI)_2Cu_3SbS_3$ and $(CuI)_3Cu_2TeS_3$ a similar situation is found with respect to the lone pair character of the metal atoms Sb and Te, respectively. Both compounds contain thiometalate units $[MS_3]^{n-}$ (M = Sb, Te) which are isolated from each other by the surrounding copper halide matrix (12, 13). Contrary to $CuClCu_2TeS_3$ the copper iodide containing compounds show a severe disorder of the copper atoms, i.e., copper is distributed over numerous sites which are not fully occupied. The coordination numbers for copper are three and four, respectively. For $(CuI)_2Cu_3SbS_3$ it was shown that the distribution of copper is temperature dependent and a reduction of the coordination number is found at low temperatures. Figure 2 shows the crystal structures of these materials. Both compounds can be regarded as built up from polyanionic layers $^2_\infty[Cu_3MS_3I_2]^{n-}$ which are shown in Figs. 2 and 3. The pronounced disorder of the copper atoms in $(CuI)_3Cu_2TeS_3$ has already been discussed (12) and will be neglected here for clarity. At a first glance these layers seem to be very similar, but a detailed analysis reveals the differences. The similarity of the layers becomes immediately obvious from their translational periods, i.e., 7.32 and 12.62 Å for $(CuI)_2Cu_3SbS_3$ vs 7.22 and 12.51 Å (orthohexagonal setting) for $(CuI)_3Cu_2TeS_3$. The slight difference is probably due to the different M–S bond lengths. Both layers consist of two different ribbons, that is, one layer of three-coordinate M and Cu atoms, and a second ribbon of four-coordinate Cu atoms. The three-coordinate atoms are surrounded either exclusively by sulfur atoms (M) or by two sulfur atoms and one iodine atom (Cu). These

TABLE 2
Comparison of Refined Model Parameters of $CuClCu_2TeS_3$[a]

	(a)	(b)	(c)
a [Å]	7.361(1)	7.3502(1)	7.3502(1)
c [Å]	10.401(1)	10.3872(2)	10.3873(2)
x(Cu)	0.52391(5)	0.52391	0.5231(1)
z(Cu)	0.24593(4)	0.24593	0.2453(3)
z(Cl)	0.5705(1)	0.5705	0.5691(4)
x(S)	0.50292(5)	0.50292	0.5031(2)
z(S)	0.47146(7)	0.47146	0.4703(4)
U_{iso}(Cu) [Å^2]	0.0249(1)	0.0249	0.0289(5)
U_{iso}(Cl) [Å^2]	0.0172(2)	0.0172	0.0159(7)
U_{iso}(Te) [Å^2]	0.01354(8)	0.01354	0.0165(9)
U_{iso}(S) [Å^2]	0.0138(2)	0.0138	0.0129(9)
Cl fraction on 3a	1.0	0.993(4)	1.001(5)
R_{wp} [%]		3.9	3.6
R_{Bragg} [%]		3.2	2.7

[a](a) Parameters from single-crystal X-ray refinement; (b) parameters from neutron refinement, release of lattice constants and Cl/S occupancies; (c) parameters from neutron refinement, release of all parameters.

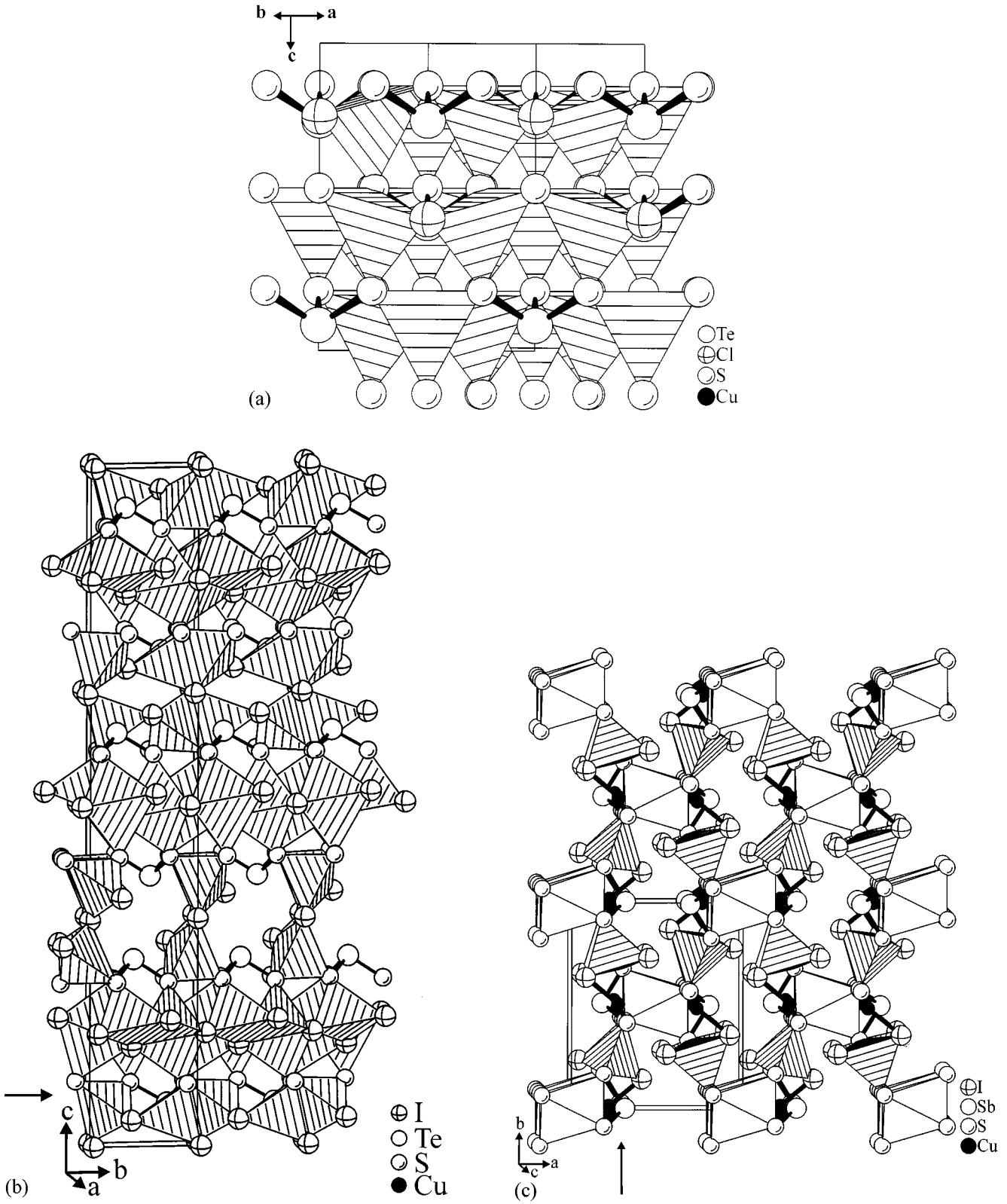

FIG. 2. Crystal structures of (a) $CuClCu_2TeS_3$ with tetrahedrally coordinated copper atoms, (b) $(CuI)_3Cu_2TeS_3$ showing a polyhedral representation exclusively of the four-coordinate copper atoms, and (c) $(CuI)_2Cu_3SbS_3$. Note that the octahedral voids in $(CuI)_2Cu_3SbS_3$ are not occupied by copper. Arrows mark the polyanionic layers shown in Fig. 3.

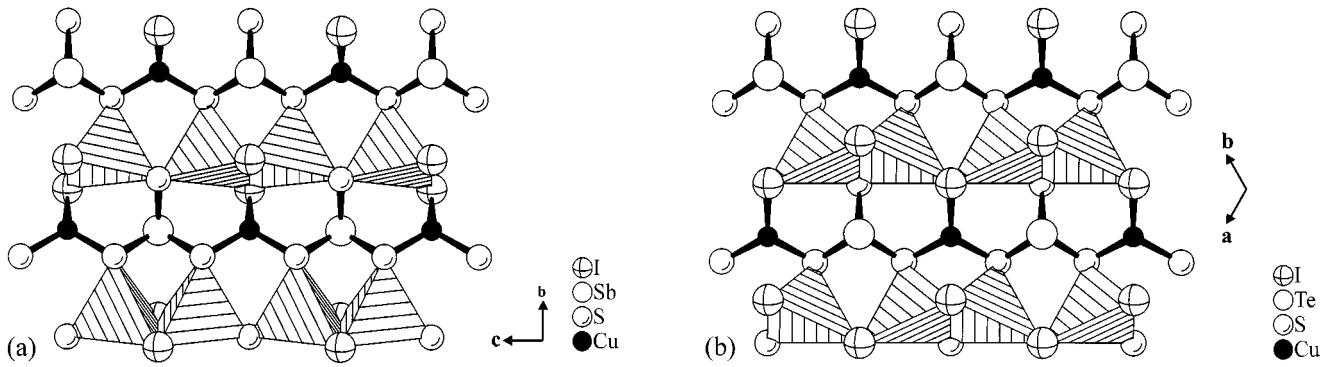

FIG. 3. Polyanionic layers $^2_\infty[Cu_3MS_3I_2]^{n-}$ in (a) $(CuI)_2Cu_3SbS_3$ and (b) $(CuI)_3Cu_2TeS_3$. At first glance the layers look similar, but they do exhibit several differences in detail.

polyhedra are interlinked by the sulfur atoms to the above mentioned ribbons. A second type of ribbons running parallel to the aforementioned ones consists of copper atoms which are coordinated by two sulfur atoms and two iodine atoms. These distorted tetrahedra $[CuS_2I_2]$ are sharing common edges to give double tetrahedra which are linked by common vertices.

The differences between the two-dimensional (2D) polyanions found in $(CuI)_2Cu_3SbS_3$ and in $(CuI)_3Cu_2TeS_3$ are due both to the $[MS_3]^{n-}$ ions and to the $[CuS_2I_2]$ ribbons. In $(CuI)_2Cu_3SbS_3$ the orientation of the $[SbS_3]^{3-}$ thiometalate ions with respect to a given layer is the same in one ribbon, but their orientation is reversed between two parallel ribbons. Contrary all $[TeS_3]^{2-}$ ions in $(CuI)_3Cu_2TeS_3$ have the same orientation in a given layer but adjacent layers have different orientations. When averaged over the whole cell, half of the thiometalate ions point "up" and the other half point "down" in both structures. The second difference between the layers is the arrangement of the sulfur atoms and the iodine atoms in the $[CuS_2I_2]$ tetrahedra. Thus, the common edges are either formed by two iodine atoms and the common vertices are sulfur atoms or the common edges are formed by one sulfur atom and one iodine atom with iodine atoms linking the double tetrahedra, cf. Fig. 3. As a result the *M* atom is bonded to three tetrahedra vertices in $(CuI)_2Cu_3SbS_3$ but to two vertices and to one common edge in $(CuI)_3Cu_2TeS_3$.

These differences in the 2D arrangement of the layers combined with their different charges $n-$ result in a completely different three-dimensional (3D) setup of the crystal structures of the compounds under discussion. In the case of $(CuI)_2Cu_3SbS_3$ the layers are arranged in a way that $[SbS_3]^{3-}$ units of adjacent layers form distorted octahedral voids. The two copper atoms which are not embedded in the layers are disordered on the faces of these octahedra. No electron density which might be due to a copper atom is found within these S_6 octahedra. The polyanionic layers $^2_\infty[Cu_3MS_3I_2]^{n-}$ of $(CuI)_3Cu_2TeS_3$ bear a formal charge of $n = 1$ due to the oxidation state $4+$ of Te as compared to $3+$ of Sb. Since two Cu^{1+} are still available an additional iodide ion is necessary for charge balance. These iodide ions are located between the layers $^2_\infty[Cu_3TeS_3I_2]^{1-}$ and are surrounded by the disordered copper atoms. Thus, the layers are not separated by octahedral voids S_6 but a large number of positions providing low coordination numbers for copper ions result. The resulting ionic conductivity and the observed activation energy can be readily interpreted as a consequence of the 3D crystal structures of the compounds under discussion, *vide infra.*

CONDUCTIVITY MEASUREMENTS

The electrical conductivity of the title compounds was determined by temperature dependent impedance spectroscopic measurements of cold pressed powder samples. Since blocking electrodes were used, these investigations provide the specific conductance and in addition they allow to conclude on the nature of charge carriers, i.e., a decision is possible whether the conductivity is predominantly ionic or electronic in nature. Figure 4 shows typical impedance spectra for $CuClCu_2TeS_3$, $(CuI)_2Cu_3SbS_3$, and $(CuI)_3Cu_2TeS_3$. Whereas the impedance spectrum of $CuClCu_2TeS_3$ shows only a semicircle, the spectra of $(CuI)_2Cu_3SbS_3$ and $(CuI)_3Cu_2TeS_3$ consist of a semicircle at high frequencies and in addition a linear spike at low frequencies. This spike is typical for ionic conductors when the measurements are performed using blocking electrodes. Thus it can be concluded from the spectra that the conductance of $CuClCu_2TeS_3$ is predominantly electronic whereas the conductivity of $(CuI)_2Cu_3SbS_3$ and $(CuI)_3Cu_2TeS_3$ is predominantly ionic. Figure 5 displays the temperature dependent evolution of the conductivities. All three compounds exhibit an increasing conductivity with rising

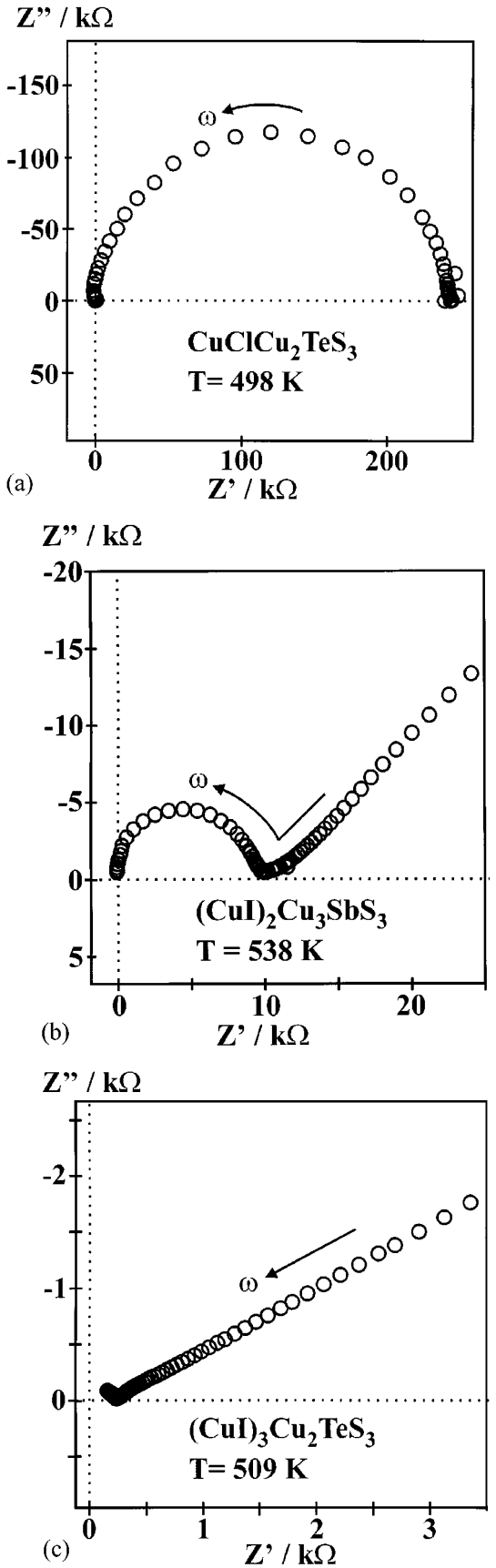

temperature. For $(CuI)_2Cu_3SbS_3$ and $(CuI)_3Cu_2TeS_3$ a pure linear dependence of log σ vs $1/T$ if observed, whereas two linear regions are found for $CuClCu_2TeS_3$. The activation energies are 0.2 eV ($(CuI)_3Cu_2TeS_3$) and 0.35 eV ($(CuI)_2Cu_3SbS_3$), respectively, for the ionic conductors. For semiconducting $CuClCu_2TeS_3$ the activation energy is 0.75 eV in the low-temperature region and 1.25 eV in the high-temperature region, *vide infra*. In addition, the specific conductivities are about four orders of magnitude higher for the copper iodide containing materials as compared to the copper chloride based compound. Due to the strong anisotropy of the crystallites of $(CuI)_3Cu_2TeS_3$ a slight variation of the conductivity data is found for different specimen. The variation of the conductance might be due to preferred orientation of the 2D shape crystallites in the specimen. Specific ionic conductivities are $6.2 \times 10^{-5}\,\Omega^{-1}\,cm^{-1}$ (50°C) and $1.9 \times 10^{-3}\,\Omega^{-1}\,cm^{-1}$ (200°C) for $(CuI)_2Cu_3SbS_3$, and $6.0 \times 10^{-4}\,\Omega^{-1}\,cm^{-1}$ (50°C) and $3 \times 10^{-3}\,\Omega^{-1}\,cm^{-1}$ (200°C) for $(CuI)_3Cu_2TeS_3$. At higher temperatures the conductivity of $(CuI)_2Cu_3SbS_3$ becomes higher than that of $(CuI)_3Cu_2TeS_3$ which is due to the lower activation energy of the latter compound. Specific conductivity data of semiconducting $CuClCu_2TeS_3$ are $10^{-7}\,\Omega^{-1}\,cm^{-1}$ (160°C) and $10^{-5}\,\Omega^{-1}\,cm^{-1}$ (280°C). The change in the slope of the Arrhenius type presentation of the conductivity of $CuClCu_2TeS_3$ at about 200°C is probably due to a phase transition. DTA measurements of $CuClCu_2TeS_3$ show a small reversible effect at about 200°C. The elucidation of the corresponding structural changes by diffraction methods is in progress.

CONCLUSION

The present investigations show that composite compounds based on copper halides and copper chalcogenides are interesting materials in terms of their electrical properties. In the case of $(CuI)_2Cu_3SbS_3$ and $(CuI)_3Cu_2TeS_3$ the electrical conductivity is mainly ionic in nature whereas $CuClCu_2TeS_3$ shows semiconducting behavior. On the one hand this difference is certainly due to changes in the electronic structure if iodine is substituted by chlorine. On the other hand the influence of the crystal structures becomes evident too. Obviously the combination of sulfide ions and iodine ions provides an anionic framework which is highly polarizable and therefore makes ionic motion possible. Combined with a large number of suitable voids low activation energies and comparably high specific conductivities

FIG. 4. Representative impedance spectra of (a) $CuClCu_2TeS_3$, (b) $(CuI)_2Cu_3SbS_3$, and (c) $(CuI)_3Cu_2TeS_3$. From the missing spike in the spectrum of $CuClCu_2TeS_3$ it can be concluded that this material exhibits predominantly electronic conduction, whereas $(CuI)_2Cu_3SbS_3$ and $(CuI)_3Cu_2TeS_3$ are ionic conducting materials.

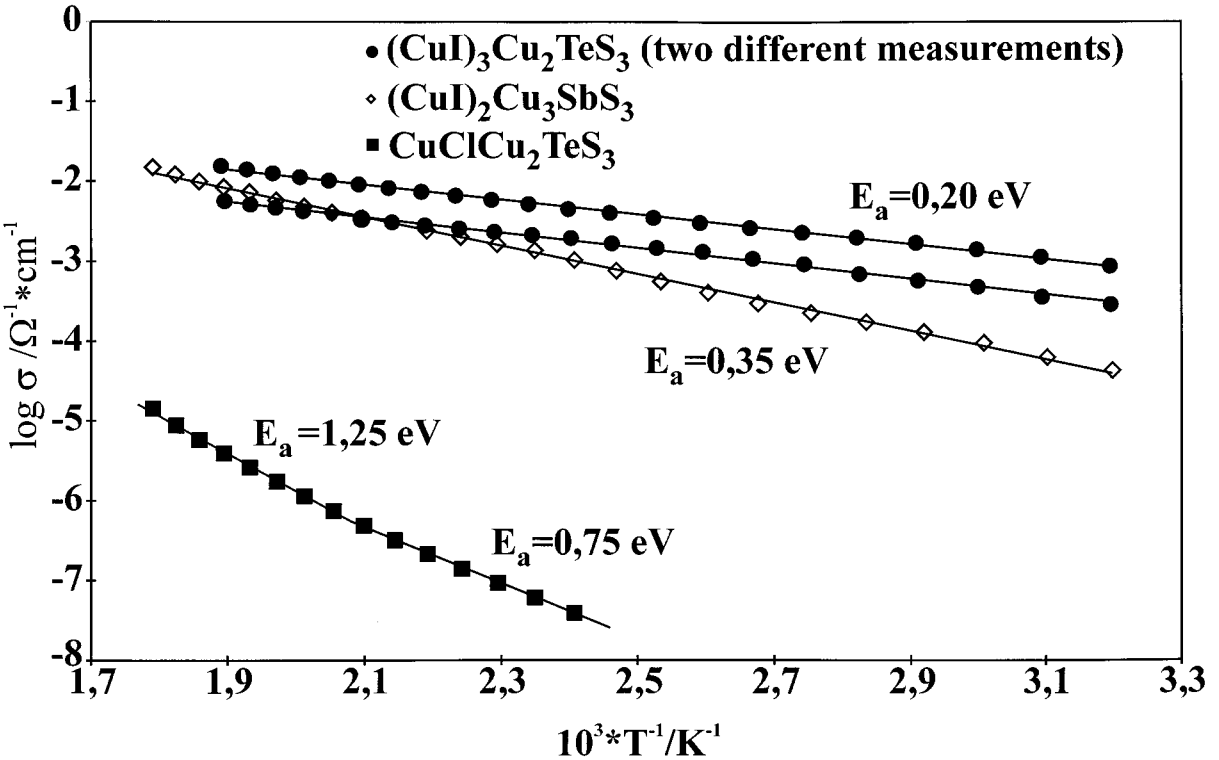

FIG. 5. Arrhenius type representation of the specific conductivities of the title compounds. Note that $CuClCu_2TeS_3$ is a semiconductor and that $(CuI)_2Cu_3SbS_3$ and $(CuI)_3Cu_2TeS_3$ are ionic conductors.

result for $(CuI)_2Cu_3SbS_3$ and $(CuI)_3Cu_2TeS_3$. Despite the fact that the polyanionic layers in $(CuI)_3Cu_2TeS_3$ and in $(CuI)_2Cu_3SbS_3$ are very similar the specific conductivity of the former compound is higher in the low-temperature region. This is certainly due to the octahedral voids in $(CuI)_2Cu_3SbS_3$ which are known to be bottlenecks for the motion of copper ions in such materials (9).

ACKNOWLEDGMENTS

The authors gratefully acknowledge the continuous support by Prof. Deiseroth and financial help by the DFG, the Fonds der Chemischen Industrie, and the BMBF, Bonn, under Contract No. KI5BO2.

REFERENCES

1. M. H. Möller and W. Jeitschko, *J. Solid State Chem.* **65,** 178 (1986).
2. E. Freudenthaler, A. Pfitzner, and D. C. Sinclair, *Mater. Res. Bull.* **31**(2), 171 (1996).
3. E. Freudenthaler and A. Pfitzner, *Solid State Ionics* **101–103,** 1053 (1997).
4. W. Truthe, *Z. Anorg. Allg. Chem.* **76,** 161 (1912).
5. G. G. Urasov and L. A. Celidse, *Izvest. Akad. Nauk. SSSR, Sekt. Fiz. Chim. Anal.* **13,** 263 (1940).
6. A. Pfitzner and S. Zimmerer, unpublished results.
7. A. Pfitzner, *Z. Anorg. Allg. Chem.* **620,** 1992 (1994).
8. E. Makovicky and T. Balic-Zunic, *Can. Mineral.* **33,** 655 (1995).
9. A. Pfitzner, *Z. Kristallogr.* **213,** 228 (1998).
10. N. F. Lugakov, A. S. Lyashevich, E. A. Movchanskii, I. I. Pokrovskii, and I. E. Shimanovich, *Dokl. Acad. Nauk B. SSR* **18,** 825 (1974).
11. M. G. Kanatzidis and A. C. Sutorki, *Prog. Inorg. Chem.* **43,** 151 (1995).
12. A. Pfitzner and S. Zimmerer, *Angew. Chem., Int. Ed. Engl.* **36,** 982 (1997).
13. A. Pfitzner, *Chem. Eur. J.* **3,** 2032 (1997).
14. A. Pfitzner, *Inorg. Chem.* **37,** 5164 (1998).
15. A. Pfitzner, F. Baumann, and W. Kaim, *Angew. Chem. Int. Ed. Eng.* **37,** 1955 (1998).
16. A. Pfitzner and T. Nilges, unpublished results.
17. W. Schäfer, E. Jansen, R. Skowronek, G. Will, W. Kockelmann, W. Schmidt, and H. Tietze-Jaensch, *Nucl. Instrum. Methods A* **364,** 179 (1995).
18. A. C. Larson and R. B. van Dreele "GSAS: General Structure Analysis System." Los Alamos National Laboratory, Los Alamos, NM, 1994.